HIF-1α is a “Brake” in JNK3 Mediated Activation of Amyloid Protein Precursor and Hyperphosphorylation of Tau Induced by T-2 Toxin in BV2 Cells

Yingying Zhao
Yangtze University
Martin Valis
charles university
Xu Wang
Huazhong Agriculture University
Eugenie Nepovimova
University of Hradec Kralove: Univerzita Hradec Kralove
Qinghua Wu (wqh212@hotmail.com)
Yangtze University https://orcid.org/0000-0002-5981-2906
Kamil Kuca
University of Hradec Kralove: Univerzita Hradec Kralove

Research Article

Keywords: T-2 toxin, hypoxia-inducible factor-1α, c-Jun N-terminal kinase, amyloid precursor protein, tau

Posted Date: September 29th, 2023

DOI: https://doi.org/10.21203/rs.3.rs-3374338/v1

Version of Record: A version of this preprint was published at Mycotoxin Research on February 6th, 2024.
See the published version at https://doi.org/10.1007/s12550-024-00525-6.

Abstract

Mycotoxins have the capacity of triggering neurodegenerative conditions like Alzheimer's disease (AD), which is marked by β-amyloid (Aβ) deposition and hyperphosphorylation of tau (P-tau). However, there is no evidence of an exact molecular mechanism to prove the above point. Due to the high toxicity and broad contamination of T-2 toxin, we assessed how T-2 toxin exposure alters amyloid precursor protein (APP) and P-tau formation in BV2 cells, and determined the underlying roles of HIF-1α and JNK3 signaling. The findings revealed that T-2 toxin stimulated the expression of HIF-1α and hypoxic stress factors in addition to increasing the expression of APP and P-tau. Additionally, HIF-1α acted as a “brake” on the induction of APP and P-tau expression by negatively regulating these proteins. Notably, T-2 toxin activated JNK3 signaling, which broke this “brake” to promote the formation of APP and P-tau. Furthermore, the cytoskeleton was an essential target for T-2 toxin to exert cytotoxicity, and JNK3/HIF-1α participated in this damage. Collectively, when the T-2 toxin induces the production of APP and P-tau, JNK3 might interfere with HIF-1α's protective function. This study will provide clues for further research on the neurotoxicity of mycotoxins.

1. Introduction

T-2 toxin, a relatively common and one of the more toxic mycotoxins in nature, has been identified as a neurotoxin (Tkaczyk and Jedziniak 2021). It can enter the brain through the blood-brain barrier (BBB), where it may cause further damage by triggering oxidative stress, neuroinflammation, and even apoptosis (Dai et al. 2019; Ravindran et al. 2011). In addition to being found in cereals, molds and toxins can be found in airborne dust. Furthermore, fungi in the environment have been reported to induce neurological diseases (Nguyen et al. 2022; Eiser 2017; Bredesen 2016). For example, Finland has a high local incidence of dementia which it has been hypothesized is due at least in part to a cold and humid climate that is suitable for mold growth (Eiser 2017). In addition, it is unknown whether mycotoxins including T-2 toxin trigger the production of key toxic proteins (Aβ, P-tau) in the pathogenesis of AD, and if so, the exact mechanism involved is still unknown.

It is known that JNK3 induces AD onset mainly through the regulation of Aβ and tau proteins. Specifically, activation of JNK3 not only phosphorylates APP, thereby promoting Aβ protein production (Yoon et al. 2012; Colombo et al. 2009), but also phosphorylates tau protein at different sites (Mamun et al. 2020; Yoshida et al. 2004). it is largely unknown whether JNK3 signaling regulates changes in Aβ and P-tau expression during exposure to T-2 toxin.

Interestingly, the toxicity of mycotoxins appears closely related to hypoxia (Wu et al. 2020). Mycotoxins can alter the expression levels of hypoxia inducible factors (HIFs), which have been demonstrated in many cell lines (Raghubeer, Nagiah, and Chuturgoon 2019; Pyo, Choi, and Lee 2021; Kowalska et al. 2019). HIF-1α, a key factor in the perception of intracellular hypoxia, is bifacial. On the one hand, it is transformed into an activator of cell death under prolonged hypoxia (Iyalomhe et al. 2017). HIF-1α participates in the development of AD by promoting Aβ production as well as inflammatory responses

(Wang et al. 2021; de Lemos et al. 2013). On the other hand, it can be neuroprotective. HIF-1α reduces the expression of genes that induce neuronal cell apoptosis, improves cerebral blood flow, inhibits hypoxia-induced Aβ protein production, and helps to maintain metabolic integrity in the brain, thereby alleviating cognitive decline or development of AD (Schubert, Soucek, and Blouw 2009; Zhang et al. 2011). This raises the interesting question that HIF-1α may have an unexpected impact on T-2 toxin-mediated production of Aβ and P-tau. Notably, it has been proposed that mycotoxin-induced oxidative stress is caused by the activation of HIF-1α, which is an issue that deserves to go for further validation. Moreover, it is not clear whether T-2 toxin alters the cytoskeleton of neural cells, and whether HIF-1α and JNK3 signaling play any functions in the cytoskeleton.

BV2 cells retain a variety of morphological, phenotypic, and functional characteristics of microglia. It is a well-recognized and typical neural cell model that is applied to study neural mechanisms and the neurotoxic mechanisms of exogenous compounds (Chen et al. 2023; Pei et al. 2023; Zhang et al. 2019). Moreover, increasing studies are using this cell line for *in vitro* research on the mechanisms of AD, especially mechanism of Aβ (Tao et al. 2022; Cho et al. 2020). Therefore, we have selected BV2 cells to investigate how T-2 toxin affects APP and P-tau expression, as well as whether HIF-1α and JNK3 are involved. In addition, we explore whether T-2 toxin targets the cytoskeleton to exert its cytotoxicity. This study offers clues for the further study of mycotoxins in neurodegenerative disorders.

2. Materials and methods

2.1. Chemicals

The supplier of the dimethylsulfoxide (DMSO) was Merck Chemical Technology Co., Ltd. in Shanghai, China. Shanghai Qifa Biotechnology Co., Ltd. (Shanghai, China) supplied the T-2 toxin (TX013-1mg, powder). YC-1 (BD156695-5mg) was from Shanghai Bide Pharmaceutical Technology Co., Ltd. (Shanghai, China). We purchased SP600125 (tlrl-sp60) and reactive oxygen species (ROS) test kit (S0033S) from Beyotime Biotechnology in Shanghai, China. Anti-Tau (phospho T181) antibody (ab254409) was obtained from Abcam (Cambridge, MA, USA). Wuhan Sevier Biotechnology Co., Ltd. (Wuhan, Hubei, China) is where we obtained the anti-JNK antibody and other reagents. The Nanjing Jiancheng Bioengineering Institute (Nanjing, Jiangsu, China) provided the assay kits for the BCA, Malondialdehyde (MDA), L-Glutathione (GSH), and Superoxide Dismutase (SOD) tests. iFluor™ 488 phalloidin iFluor™ 488 labeled phalloidin (green) was originated from Yeasen Biotechnology Co., Ltd. (Shanghai, China).

2.2. BV2 cells culture

The BV2 mouse microglia line was provided by the School of Medicine, Yangtze University (Jingzhou, Hubei, China). Complete DMEM (Thermo Fisher Scientific, USA), which contains 1% (v/v) penicillin-streptomycin mixture (Solaibao, Beijing, China) with 10% (v/v) FBS (Sijiqing, Hangzhou, China), was used to culture the cells. The cells were cultivated at 37°C in a 5% CO_2 constant temperature and humidity cell

incubator after being sown onto T25 culture flasks. Cell passaging was performed when the cells were in good condition and at 80%-90% confluency.

The experiment consisted of four groups: control group, T-2 toxin-treated group, T-2 + YC-1 (10 μM), and T-2 + SP600125 (20 μM) groups, with three replicates per group. The inhibitors at this concentration had no toxic effect on the cells (data not shown). Based on the outcomes of pre-experiments, culture BV2 cells with DMEM containing 8 or 16 nM T-2 toxin for 0.5, 1, 2, 4, 8, 12, and 24 h; before being exposed to T-2 toxin, BV2 cells of both inhibitors treated groups were pretreated with specific concentrations of inhibitors (YC-1 or SP600125) for 1 h; the control group was treated with complete DMEM.

2.3. Quantitative real-time PCR

For quantitative real-time PCR (RT-PCR), we mainly refer to the test method of You et al. (2022). In brief, BV2 cells were collected after being exposed to T-2 toxin (8 nM) for 0.5–24 h, and total RNA was extracted in accordance with the RNA Extraction Kit's instructions (TIANGEN, Beijing, China). According to the instructions on the FastKing One-Step Genomic cDNA First Strand Synthesis Master Mix Kit (TIANGEN, Beijing, China), reverse transcription of the extracted RNA into cDNA was performed. Finally, RT-PCR was used to amplify the cDNA. In Table 1, primer sequences are displayed.

Table 1
Primer sequences for RT-PCR.

Gene	Sequence (5′-3′)	bps
GPx-1	Fwd: GAAGGTAAAGAGCGGGTGA	133
	Rev: GGAGAATGGCAAGAATGAAG	
CAT	Fwd: GTGTTGAACGAGGAGGAGAG	195
	Rev: CTGCGTGTAGGTGTGAATTG	
SOD-2	Fwd: AGGAGAGTTGCTGGAGGCTATCAAG	157
	Rev: ATTAGAGCAGGCGGCAATCTGTAAG	
APP	Fwd: TGAATGTGCAGAATGGAAAGTG	224
	Rev: AACTAGGCAACGGTAAGGAATC	
PSEN1	Fwd: GCCCCAGAGTAACTCAAGACA	163
	Rev: CCGGGTATAGAAGCTGACTGA	
Tau	Fwd: GACATGGACCATGGCTTAAAAG	134
	Rev: GCTTTCTTCTCGTCATTTCCTG	
JNK3	Fwd: TGAAGAAATTGCAGCCCACC	180
	Rev: TCTTCGCTGGGTCAATCACT	
VEGF	Fwd: TATTCAGCGGACTCACCAGC	156
	Rev: AACCAACCTCCTCAAACCGT	
LDHA	Fwd: GCTTCCATTTAAGGCCCCG	275
	Rev: TCATCCGCCAAGTCCTTCAT	
PDK1	Fwd: GGACTTCGGGTCAGTGAATGC	122
	Rev: TCCTGAGAAGATTGTCGGGGA	
HIF-1α	Fwd: GAATGAAGTGCACCCTAACAAG	177
	Rev: GAGGAATGGGTTCACAAATCAG	
GAPDH	Fwd: AACTTTGGCATTGTGGAAGG	223
	Rev: ACACATTGGGGGTAGGAACA	

2.4. Western blot analysis

BV2 cells were obtained after being exposed to T-2 toxin (8 nM) for 1 or 8 h, and they were then given three washes with normothermic PBS. We used our prior experimental method for western blot analysis

(You et al. 2022). In simple terms, cells were lysed with cell lysis solution (RIPA lysis solution + 1 mM PMSF + 1% protease inhibitor + 1 mM sodium orthovanadate) at low temperature for 30 min, followed by centrifugation at 5,000 ×g for 15 min at 4°C. The BCA approach was used to evaluate each sample's protein concentration. Then, the concentration of each group of protein samples was adjusted to the same concentration using 5×SDS-PAGE protein loading buffer, followed by 8 min of boiling in a water bath at 100°C. Subsequently, electrophoresis was performed and the PAGE gels were removed and transferred immediately. The membranes were placed on a decolorization shaker and incubated with 5% defatted milk powder for 1 h, then exposed to primary and secondary antibodies and washed with TBST solution. Chemiluminescence was performed with ECL solution. Eventually, the image was loaded with Sensi Ansys image analysis software, the data was saved and sorted, and then the images were decolorized with Photoshop prior to densitometry.

2.5. Determination of intracellular ROS and oxidative stress marker levels

Martinez et al. (2021)'s approach was primarily used to measure the formation of ROS. T-2 toxin (8 or 16 nM) was used to treat BV2 cells for 12 h, and the probe was loaded into the cell suspension according to the instructions of the kit. Then, cells were gently blown down with pre-cooled PBS and collected into a dark-colored 96-well plate. On a fluorescence microplate reader (Bio-Rad), the fluorescence was detected once in 5 min for a total of 30 min. Detection conditions: the fluorescence intensity at 525 nm emission wavelength was detected under 488 nm excitation. Finally, the percentage of fluorescence increase per well was calculated.

MDA, SOD and GSH content and activities in the cells were determined by collecting and analyzing the supernatant after the treatment of the above cell samples, in accordance with the instructions provided with each kit.

2.6. Detection of cytoskeleton by phalloidin fluorescent labeling

The nuclei and cytoskeleton of the cells were stained in accordance with the kit's instructions after T-2 toxin (8 nM) treatment for 12 h. Under a fluorescence microscope (Olympus, Japan), the fluorescence was seen and captured on camera. iFluor™ 488: the fluorescence intensity at 517 nm emission wavelength was detected under 493 nm excitation. DAPI: the fluorescence intensity at 454 nm emission wavelength was detected under 364 nm excitation. Finally, to evaluate the fluorescence intensity, Image-Pro Plus 6.0 was used.

2.7. Statistical analysis

SPSS 22.0 was used for statistical analysis. Each experiment was done three times independently (n = 3), with the data being represented by mean ± standard deviation (SD). By using one-way ANOVA, the difference between the groups was evaluated. $p < 0.05$ indicates significant differences, and $p < 0.01$ indicates highly significant differences. F values and degrees of freedom were analyzed as well.

3. Results

3.1. JNK3 signaling plays a crucial role in T-2 toxin-induced expression of APP and P-tau

To probe the kinetics of expression of key genes in AD, after 0.5–24 h of T-2 toxin exposure, we detected *APP*, *PSEN1* and microtubule-associated protein tau gene (*Mapt*) expression in microglia. We demonstrated that the peak expression of *APP*, *PSEN1* and *Mapt* (encoding tau) occurred at 8 h (Fig. 1). Therefore, in subsequent inhibitor experiments, we chose the T-2 toxin to act for 8 h. According to the genetic results of the inhibitor assay, the expression of *APP*, *PSEN1*, and *Mapt* was higher in the T-2 toxin group than it was in the control group (Fig. 2). Western blot analysis further indicated the same results (Fig. 3C and D). Moreover, we found that JNK3 signaling had detectable activity within 1 h of T-2 toxin exposure and reached its highest expression at 8 h (Fig. 1). Since study findings have proven that JNK3 is essential for the occurrence of AD, we explored the role played by JNK3 signaling in the upregulation of APP and tau expression after exposure to T-2 toxin. Our investigations proved that JNK3 inhibited *Mapt* expression while promoting *APP* and *PSEN1* expression when the T-2 toxin was present (Fig. 2). At the protein level, JNK3 promoted T-2 toxin-induced APP protein expression but suppressed the phosphorylation level of tau protein induced via T-2 toxin (Fig. 3C and D). The above findings suggested that JNK3 controls APP and P-tau expression in the context of the toxicity exerted via T-2 toxin.

In addition, cellular oxidative stress was explored as part of the neurotoxicity exerted via T-2 toxin. The findings elucidated that the gene expression of *CAT* and *SOD-2* peaked at 8 h of T-2 toxin action, while *Gpx-1* kept rising after 8 h (Fig. 1). T-2 toxin made the antioxidant enzyme SOD more active, and MDA and ROS levels were similarly elevated, but GSH levels were reduced (Fig. 4). All of the above were toxin concentration dependent.

3.2. T-2 toxin activated HIF-1α and hypoxia stress reaction

To investigate the effects of T-2 toxin exposure on the expression of HIF-1α, as well as to ascertain whether it increases hypoxic stress factors (VEGF, PDK1, LDHA) expression, we validated this at the gene and protein levels, respectively. Our research results demonstrated that significant expression of *HIF-1α* was seen at 1 h of T-2 toxin exposure, followed by decreasing expression (Fig. 1). Subsequently, hypoxic stress factors hypoxic stress factors were activated and reached its highest expression at 8 h of toxin exposure (Fig. 1), and thus we examined their expression at 8 h of toxin action in inhibitor experiments (Fig. 2). When HIF-1α was inhibited, the expression of *VEGF*, *PDK1* and *LDHA* were all downregulated to varying degrees (0.75- to 1.4-fold) (Fig. 2), which demonstrated that *VEGF*, *PDK1* and *LDHA* were downstream factors of HIF-1α. Therefore, we proved that T-2 toxin exposure could rapidly promote HIF-1α expression and activate its downstream factors in BV2 cells.

To explore whether JNK3 signaling is associated with HIF-1α induced via T-2 toxin, we examined the expression of HIF-1α and HIF-1 target genes after inhibition of JNK3 signaling. We showed that activation

of JNK3 signaling had a remarkably inhibitory effect on HIF-1α expression (Fig. 2 and Fig. 3A). Among these downstream factors, JNK3 had an inhibitory effect on *LDHA* (Fig. 2) but a promoting effect on VEGF (Fig. 3B) and *PDK1* (Fig. 2). Hence, we suspect that JNK3 inhibits HIF-1α by regulating hypoxic stress factors.

3.3. HIF-1α is a “brake” in JNK3 mediated APP and P-tau expression

To investigate what function HIF-1α signaling plays in T-2 toxin-induced APP and P-tau protein production, we observed the expression levels of the above two proteins in the presence of inhibition of HIF-1α signaling. We discovered that HIF-1α significantly negatively regulates T-2 toxin-mediated expression of APP protein and P-tau (Fig. 2 and Fig. 3C, D). Notably, HIF-1α signaling and JNK3 signaling are mutually inhibited (Fig. 2 and Fig. 3E). Therefore, we speculate that HIF-1α may act as a “brake” in T-2 toxin-induced expression of APP and P-tau by inhibiting JNK3 signaling. However, in this study, it seems that JNK3 broke the effects of the “brake” (HIF-1α) to promote the formation of APP and P-tau in the presence of T-2 toxin action.

We further investigated the function of HIF-1α signaling in T-2 toxin-induced oxidative stress since oxidative stress and HIF-1α are closely related. HIF-1α signaling was inhibited to investigate its role in T-2 toxin-mediated oxidative stress. We found that HIF-1α promoted antioxidant GSH and SOD levels (Fig. 4A and D) in addition to increasing ROS and MDA levels produced via T-2 toxin (Fig. 4B and C), proving that HIF-1α has a dual effect in the stimulation of T-2 toxin exposure. Meanwhile, we established that JNK3 promoted the formation of ROS and MDA caused via T-2 toxin (Fig. 4A and D), while reducing the activities of antioxidant enzymes (GSH, SOD) by regulating the editing genes (*CAT*, *Gpx-1*, *SOD-2*) of antioxidant enzymes (Fig. 2), demonstrating that JNK3 signaling had a complete promoting effect on T-2 toxin-mediated oxidative damage in BV2 cells.

3.4. JNK3/HIF-1α activation promotes BV2 cytoskeletal damage

To explore whether the cytoskeleton is a major target for T-2 toxin to exert cytotoxicity, we examined changes in the BV2 cytoskeleton by immunofluorescence, and explored the effects of JNK3 and HIF-1α on these changes. We showed that the control cells were regular and round, and of a uniform size, the cell membrane was intact, the cells were plump, the surface did not have obvious cell protrusions, and the fluorescence staining was uniform with high brightness (Fig. 5A). However, the cells in the toxin-treated group had irregular morphology, displayed significantly weaker and uneven fluorescence staining, and were marked by budding and dendritic irregular protrusions on the cell surface, which indicated that T-2 toxin could destroy cytoskeleton (Fig. 5A and B). When the activity of JNK3 and HIF-1α was inhibited, the cytoskeleton was partially restored. Most of the cells were round, and the fluorescent staining was

noticeably brighter than observed in the toxin group (Fig. 5A and B), suggesting that JNK3 and HIF-1α contributed to the T-2 toxin-mediated cytoskeletal damage.

4. Discussion

Research has shown that *APP* and *PSEN1* gene are pathogenic genes strongly associated with AD pathogenesis, with *PSEN1* carrying the largest number of pathogenic variants (Xiao et al. 2021). PSEN1, as a subunit of γ-secretase, can bind to the γ-secretase site in the transmembrane structural domain of APP, thus promoting the production of Aβ protein (Escamilla-Ayala et al. 2020; Esselens et al. 2012). It is unclear if T-2 toxin affects these pathogenic genes and contributes to the onset of AD. Hence, we explored how the T-2 toxin affected the expression of the *APP* and *PSEN1* genes. T-2 toxin greatly increased the expression of the genes for *APP* and *PSEN1*, which suggests that it may have a role in the pathogenesis of AD. Indeed, elevated APP expression was detected in the brain tissue of APP/PS1 double transgenic mice (Jankowsky et al. 2004). Moreover, it has been established that *Mapt* is closely associated with neurodegeneration and that P-tau proteins is one of the key causative factors in AD (Zhang et al. 2016). Thus, we examined the expression levels of *Mapt* and P-tau proteins during T-2 toxin exposure. According to the findings, T-2 toxin markedly elevated *Mapt* expression and tau protein phosphorylation.

We further explored JNK3's function in APP and P-tau expression induced via T-2 toxin. Our research indicated that T-2 toxin greatly activated JNK3. Upon inhibition of JNK3 signaling, APP and P-tau expression were downregulated, suggesting that JNK3 signaling participated in T-2 toxin-mediated neurotoxicity. Earlier studies have demonstrated that JNK phosphorylates APP and tau, leading to the formation of extra-neuronal senile plaques and intra-neuronal neurofibrillary tangles, and ultimately promoting the development of AD (Zhao et al. 2022). Consistent with this, we showed that JNK3 promoted the production of the APP protein caused via T-2 toxin. However, our study further showed that JNK3 inhibits the phosphorylation of tau protein caused via T-2 toxin. This result differs from previous studies, which may suggest that JNK3 has an inhibitory effect on AD development under certain circumstances, for example, according to the exposure time and dose of exogenous compounds.

Mycotoxin-induced changes in HIF-1α expression have been found in different *in vitro* model studies (Habrowska-Gorczynska et al. 2019; Raghubeer, Nagiah, and Chuturgoon 2019; Kowalska et al. 2019). Therefore, HIF-1α signaling is considered to play a mediating role in mycotoxin signaling. However, prior studies only focused on changes of HIF-1α expression; its mechanism of action in mycotoxin-induced neurotoxicity has never been explored. Our research demonstrated that T-2 toxin stimulated HIF-1α in BV2 cells. Moreover, T-2 toxin enhanced VEGF expression, as well as glycolytic enzyme genes *PDK1* and *LDHA*. Among these, PDK1 is essential for organismal adaptation to metabolic stressors (Dupuy et al. 2015). Thus, our findings suggested that T-2 toxin could regulate glycolysis and promote angiogenesis in BV2 cells as part of an adaptation to hypoxia. In addition, other investigations have demonstrated that HIF-1α, PDK1 and LDHA are expressed in HepG2 cells after 6 h of exposure to different doses of fusaric acid (FA), which coincides with our research findings (Sheik Abdul, Nagiah, and Chuturgoon 2020). In

short, our findings showed that T-2 toxin promotes HIF-1α expression and activates HIF-1 target genes in BV2 cells.

Under conditions of moderate hypoxia, HIF-1α would positively regulate multiple regulatory factors, including VEGF, PDK1, LDHA, thus allowing cells to survive in hypoxic circumstances (Sankar, Altamentova, and Rocheleau 2019). In this research, we found that the expression of *VEGF*, *PDK1* and *LDHA* was decreased after HIF-1α activity was inhibited. This indicated that VEGF, PDK1 and LDHA may act downstream of HIF-1α signaling in response to cellular hypoxia mediated by exposure to T-2 toxin, and contribute to HIF-1α as part of a protective pathway regulating cellular adaptation to hypoxia. Specifically, HIF-1α positively regulated the expression of VEGF, thereby promoting angiogenesis. It also positively regulated the expression of glycolytic enzyme genes (*PDK1*, *LDHA*), which allow cells to synthesize adenosine triphosphate in an oxygen independent manner. Therefore, HIF-1α seems to be part of a metabolic regulatory system of T-2 toxin-stimulated cells, promoting the transcription of concentrated glycolytic enzymes. Similarly, previous research revealed that HIF-1 can enhance local microcirculation by influencing blood vessel development and function as well as control oxygen uptake by switching from oxidative to glycolytic metabolism (Semenza 2011; Sheik Abdul, Nagiah, and Chuturgoon 2020; Shohet and Garcia 2007). Interestingly, we found that JNK3 inhibits the expression of HIF-1α and regulates the expression levels of downstream target genes (*VEGF*, *PDK1* and *LDHA*) of HIF-1. Therefore, we speculate that JNK3 may achieve its inhibitory effect on HIF-1α signaling by regulating the downstream factors of HIF-1α. Moreover, under hypoxic conditions, mitochondria produce large amounts of ROS, which will induce the body to produce a hypoxia stress reaction, so HIF-1α is activated as response to hypoxia (Li et al. 2014). Our research suggested that T-2 toxin not only induced intracellular ROS generation as well as lipid peroxidation, but also activated the antioxidant system. Wu et al. (2020) have proposed that activation of HIF-1α is a factor in the oxidative stress caused by mycotoxin. Our findings, which are consistent with the prior studies, indicated that HIF-1α promoted the generation of ROS and MDA via T-2 toxin. Importantly, we found that HIF-1α increased the activities of the antioxidant factors GSH and SOD, demonstrating that HIF-1α plays a dual role in oxidative stress brought on the T-2 toxin. The two-sided nature of the HIF-1α pathway was highlighted in previous studies: it protects neurons from mild hypoxia, but not from prolonged hypoxia (Merelli et al. 2018; Lopez-Hernandez et al. 2012).

According to earlier studies, excessive HIF-1α expression increases the expression of β-secretase through overexpression of β-secretase β site APP cleavage enzyme 1 (BACE1), thereby inducing APP proteolytic processing to produce Aβ protein and ultimately promoting the pathogenesis of AD (Merelli et al. 2018; Sun et al. 2006; Zhang et al. 2007). Interestingly, contrary to the earlier findings, we found that HIF-1α inhibited APP expression and phosphorylation of tau protein resulting from T-2 toxin (Fig. 3C and D), as well as suppressed *PSEN1* gene expression (Fig. 2), indicating that HIF-1α is part of a protective pathway that regulates expression of APP and P-tau mediated by T-2 toxin. Under hypoxic conditions, HIF-1α was found to increase oxygen delivery and supply by inducing erythrocytes and angiogenesis (we also offer supporting evidence for this in this study), to inhibit hypoxia-induced Aβ protein production, and help maintain metabolic integrity in the brain, to reduce the P-tau expression, and to delay the onset of AD (Zhang et al. 2011; Wang et al. 2021; Schubert, Soucek, and Blouw 2009). Furthermore, our results further

uncovered a reciprocal inhibitory relationship between JNK3 and HIF-1α signaling. We speculate that HIF-1α may conduct negative regulatory effect on APP and P-tau expression by inhibiting JNK3 signaling, just like a “brake” of a car. Notably, JNK3 broke this “brake” (HIF-1α), and thereby participated in the production of APP and P-tau.

T-2 toxin has strong immunotoxicity, yet its effects on cell structure, especially the cytoskeleton, have been rarely reported (Wu et al. 2014). We first observed that T-2 toxin could affect the function of BV2 cells by damaging the cytoskeletal structure, and found that JNK3/HIF-1α signaling participated in the process of cytoskeleton damage. This implicated that T-2 toxin effect on BV2 cells is directed towards the cytoskeleton. We further suggested that the cytoskeletal damage mediated by JNK3/HIF-1α may have a relationship with the expression of Aβ and tau, as all these negative indicators are controlled by JNK3 in this context.

In conclusion, we demonstrated that T-2 toxin resulted in upregulated expression levels of APP and P-tau in BV2 cells, which may be the target of T-2 toxin's action in the pathogenesis of AD. We also discovered that T-2 toxin activated JNK3 and HIF-1α rapidly. Interestingly, We discovered that HIF-1α negatively regulated the expression of APP and P-tau, suggesting that it provided protection against the cytotoxicity caused via T-2 toxin. Notably, JNK3 appeared to undermine this protective function, contributing to the T-2 toxin's ability to trigger the production of APP and P-tau. It was discovered that JNK3 and HIF-1α both played a part in the disruption of the cytoskeleton caused by T-2 toxin. All the above conjectures are shown in Fig. 6. This research provides a mechanistic perspective for further studies on the mechanisms of neurotoxicity involved in T-2 toxin.

Declarations

Funding

This work was supported by the National Natural Science Foundation of China (Grant nos. 31972741; 32373073; 32072925), MH CZ-DRO (UHHK, 00179906), Research program of University of Granada, by the Charles University in Prague, Czechia (PROGRES Q40/15) and the Excellence project PrF UHK 2217/2022-2023Czech Republic.

CRediT authorship contribution statement

Yingying Zhao performed the experiment, and drafted the manuscript. Martin Valis reviewed and analyzed the data. Xu Wang and Eugenie Nepovimova contributed to the discussion and review of the manuscript. Qinghua Wu and Kamil Kuca designed the research and analyzed the data. All co-authors reviewed and edited the manuscript and approved the submission.

Acknowledgements

We would like to thank the National Natural Science Foundation of China.

Conflicts of Interest

The authors declare that they have no conflicts of interest.

References

1. Bredesen, D. E. 2016. 'Inhalational Alzheimer's disease: an unrecognized - and treatable - epidemic', *Aging (Albany NY)*, 8: 304 – 13.
2. Chen, G., M. Han, Y. Chen, Y. Lei, M. Li, L. Wang, C. Wang, Y. Hu, J. Niu, C. Yang, Y. Mo, Q. Wang, L. Yang, and X. Chang. 2023. 'Danggui-Shaoyao-San Promotes Amyloid-beta Clearance through Regulating Microglia Polarization via Trem2 in BV2 Cells', *J Integr Neurosci*, 22: 72.
3. Cho, K., Y. J. Jang, S. J. Lee, Y. N. Jeon, Y. L. Shim, J. Y. Lee, D. S. Lim, D. H. Kim, and S. Y. Yoon. 2020. 'TLQP-21 mediated activation of microglial BV2 cells promotes clearance of extracellular fibril amyloid-beta', *Biochem Biophys Res Commun*, 524: 764 – 71.
4. Colombo, A., A. Bastone, C. Ploia, A. Sclip, M. Salmona, G. Forloni, and T. Borsello. 2009. 'JNK regulates APP cleavage and degradation in a model of Alzheimer's disease', *Neurobiol Dis*, 33: 518 – 25.
5. Dai, C., X. Xiao, F. Sun, Y. Zhang, D. Hoyer, J. Shen, S. Tang, and T. Velkov. 2019. 'T-2 toxin neurotoxicity: role of oxidative stress and mitochondrial dysfunction', *Arch Toxicol*, 93: 3041-56.
6. de Lemos, Maria Luisa, Aurelio Vazquez de la Torre, Dimitry Petrov, Susana Brox, Jaume Folch, Mercè Pallàs, Alberto Lazarowski, Carlos Beas-Zarate, Carme Auladell, and Antoni Camins. 2013. 'Evaluation of hypoxia inducible factor expression in inflammatory and neurodegenerative brain models', *The International Journal of Biochemistry & Cell Biology*, 45: 1377-88.
7. Dupuy, F., S. Tabaries, S. Andrzejewski, Z. Dong, J. Blagih, M. G. Annis, A. Omeroglu, D. Gao, S. Leung, E. Amir, M. Clemons, A. Aguilar-Mahecha, M. Basik, E. E. Vincent, J. St-Pierre, R. G. Jones, and P. M. Siegel. 2015. 'PDK1-dependent metabolic reprogramming dictates metastatic potential in breast cancer', *Cell Metab*, 22: 577 – 89.
8. Eiser, A. R. 2017. 'Why does Finland have the highest dementia mortality rate? Environmental factors may be generalizable', *Brain Res*, 1671: 14–17.
9. Escamilla-Ayala, Abril, Rosanne Wouters, Ragna Sannerud, and Wim Annaert. 2020. 'Contribution of the Presenilins in the cell biology, structure and function of γ-secretase', *Seminars in Cell & Developmental Biology*, 105: 12–26.
10. Esselens, Cary, Ragna Sannerud, Rodrigo Gallardo, Veerle Baert, Daniela Kaden, Lutgarde Serneels, Bart De Strooper, Frederic Rousseau, Gerd Multhaup, Joost Schymkowitz, Johannes P. M. Langedijk, and Wim Annaert. 2012. 'Peptides based on the presenilin-APP binding domain inhibit APP processing and Aβ production through interfering with the APP transmembrane domain', *The FASEB Journal*, 26: 3765-78.
11. Habrowska-Gorczynska, D. E., K. Kowalska, K. A. Urbanek, K. Dominska, A. Sakowicz, and A. W. Piastowska-Ciesielska. 2019. 'Deoxynivalenol modulates the viability, ROS production and apoptosis

in prostate cancer cells', *Toxins (Basel)*, 11: 265.

12. Iyalomhe, O., S. Swierczek, N. Enwerem, Y. Chen, M. O. Adedeji, J. Allard, O. Ntekim, S. Johnson, K. Hughes, P. Kurian, and T. O. Obisesan. 2017. 'The role of hypoxia-inducible factor 1 in mild cognitive impairment', *Cell Mol Neurobiol*, 37: 969 – 77.
13. Jankowsky, J. L., D. J. Fadale, J. Anderson, G. M. Xu, V. Gonzales, N. A. Jenkins, N. G. Copeland, M. K. Lee, L. H. Younkin, S. L. Wagner, S. G. Younkin, and D. R. Borchelt. 2004. 'Mutant presenilins specifically elevate the levels of the 42 residue beta-amyloid peptide in vivo: evidence for augmentation of a 42-specific gamma secretase', *Human Molecular Genetics*, 13: 159 – 70.
14. Kowalska, K., D. E. Habrowska-Gorczynska, K. A. Urbanek, K. Dominska, A. Sakowicz, and A. W. Piastowska-Ciesielska. 2019. 'Estrogen receptor beta plays a protective role in zearalenone-induced oxidative stress in normal prostate epithelial cells', *Ecotoxicol Environ Saf*, 172: 504 – 13.
15. Li, Y. N., M. M. Xi, Y. Guo, C. X. Hai, W. L. Yang, and X. J. Qin. 2014. 'NADPH oxidase-mitochondria axis-derived ROS mediate arsenite-induced HIF-1alpha stabilization by inhibiting prolyl hydroxylases activity', *Toxicol Lett*, 224: 165 – 74.
16. Lopez-Hernandez, B., I. Posadas, P. Podlesniy, M. A. Abad, R. Trullas, and V. Cena. 2012. 'HIF-1alpha is neuroprotective during the early phases of mild hypoxia in rat cortical neurons', *Exp Neurol*, 233: 543 – 54.
17. Mamun, A. A., M. S. Uddin, B. Mathew, and G. M. Ashraf. 2020. 'Toxic tau: structural origins of tau aggregation in Alzheimer's disease', *Neural Regen Res*, 15: 1417-20.
18. Martinez, M. A., I. Ares, M. Martinez, B. Lopez-Torres, J. E. Maximiliano, J. L. Rodriguez, M. R. Martinez-Larranaga, A. Anadon, C. Peteiro, S. Rubino, and M. Hortos. 2021. 'Brown marine algae Gongolaria baccata extract protects Caco-2 cells from oxidative stress induced by tert-butyl hydroperoxide', *Food Chem Toxicol*, 156: 112460.
19. Merelli, A., J. C. G. Rodriguez, J. Folch, M. R. Regueiro, A. Camins, and A. Lazarowski. 2018. 'Understanding the role of hypoxia inducible factor during neurodegeneration for new therapeutics opportunities', *Curr Neuropharmacol*, 16: 1484-98.
20. Nguyen, V. T. T., S. Konig, S. Eggert, K. Endres, and S. Kins. 2022. 'The role of mycotoxins in neurodegenerative diseases: current state of the art and future perspectives of research', *Biol Chem*, 403: 3–26.
21. Pei, X., F. Hu, Z. Hu, F. Luo, X. Li, S. Xing, L. Sun, and D. Long. 2023. 'Neuroprotective Effect of alpha-Lipoic Acid against Abeta(25–35)-Induced Damage in BV2 Cells', *Molecules*, 28:1168.
22. Pyo, M. C., I. G. Choi, and K. W. Lee. 2021. 'Transcriptome Analysis Reveals the AhR, Smad2/3, and HIF-1alpha Pathways as the Mechanism of Ochratoxin A Toxicity in Kidney Cells', *Toxins (Basel)*, 13:190.
23. Raghubeer, S., S. Nagiah, and A. Chuturgoon. 2019. 'Ochratoxin A upregulates biomarkers associated with hypoxia and transformation in human kidney cells', *Toxicol In Vitro*, 57: 211 – 16.
24. Ravindran, J., M. Agrawal, N. Gupta, and P. V. Rao. 2011. 'Alteration of blood brain barrier permeability by T-2 toxin: Role of MMP-9 and inflammatory cytokines', *Toxicology*, 280: 44–52.

25. Sankar, K. S., S. M. Altamentova, and J. V. Rocheleau. 2019. 'Hypoxia induction in cultured pancreatic islets enhances endothelial cell morphology and survival while maintaining beta-cell function', *PLoS One*, 14: e0222424.
26. Schubert, D., T. Soucek, and B. Blouw. 2009. 'The induction of HIF-1 reduces astrocyte activation by amyloid beta peptide', *Eur J Neurosci*, 29: 1323-34.
27. Semenza, G. L. 2011. 'Hypoxia-inducible factor 1: regulator of mitochondrial metabolism and mediator of ischemic preconditioning', *Biochim Biophys Acta*, 1813: 1263-68.
28. Sheik Abdul, N., S. Nagiah, and A. A. Chuturgoon. 2020. 'The neglected foodborne mycotoxin Fusaric acid induces bioenergetic adaptations by switching energy metabolism from mitochondrial processes to glycolysis in a human liver (HepG2) cell line', *Toxicol Lett*, 318: 74–85.
29. Shohet, R. V., and J. A. Garcia. 2007. 'Keeping the engine primed: HIF factors as key regulators of cardiac metabolism and angiogenesis during ischemia', *J Mol Med (Berl)*, 85: 1309-15.
30. Sun, X., G. He, H. Qing, W. Zhou, F. Dobie, F. Cai, M. Staufenbiel, L. E. Huang, and W. Song. 2006. 'Hypoxia facilitates Alzheimer's disease pathogenesis by up-regulating BACE1 gene expression', *Proc Natl Acad Sci U S A*, 103: 18727-32.
31. Tao, L., M. Hu, X. Zhang, X. Wang, Y. Zhang, X. Chen, J. Tang, and J. Wang. 2022. 'Methamphetamine-mediated dissemination of beta-amyloid: Disturbances in endocytosis, transport and clearance of beta-amyloid in microglial BV2 cells', *Toxicol Appl Pharmacol*, 447: 116090.
32. Tkaczyk, A., and P. Jedziniak. 2021. 'Mycotoxin biomarkers in pigs-current state of knowledge and analytics', *Toxins (Basel)*, 13: 586.
33. Wang, Y. Y., Z. T. Huang, M. H. Yuan, F. Jing, R. L. Cai, Q. Zou, Y. S. Pu, S. Y. Wang, F. Chen, W. M. Yi, H. J. Zhang, and Z. Y. Cai. 2021. 'Role of hypoxia inducible factor-1alpha in Alzheimer's disease', *J Alzheimers Dis*, 80: 949 − 61.
34. Wu, Q., Z. Qin, K. Kuca, L. You, Y. Zhao, A. Liu, K. Musilek, Z. Chrienova, E. Nepovimova, P. Oleksak, W. Wu, and X. Wang. 2020. 'An update on T-2 toxin and its modified forms: metabolism, immunotoxicity mechanism, and human exposure assessment', *Arch Toxicol*, 94: 3645-69.
35. Wu, Q., X. Wang, D. Wan, J. Li, and Z. Yuan. 2014. 'Crosstalk of JNK1-STAT3 is critical for RAW264.7 cell survival', *Cell Signal*, 26: 2951-60.
36. Xiao, X. W., H. Liu, X. X. Liu, W. W. Zhang, S. Z. Zhang, and B. Jiao. 2021. 'APP, PSEN1, and PSEN2 Variants in Alzheimer's Disease: Systematic Re-evaluation According to ACMG Guidelines', *Frontiers in Aging Neuroscience*, 13:695808..
37. Yoon, S. O., D. J. Park, J. C. Ryu, H. G. Ozer, C. Tep, Y. J. Shin, T. H. Lim, L. Pastorino, A. J. Kunwar, J. C. Walton, A. H. Nagahara, K. P. Lu, R. J. Nelson, M. H. Tuszynski, and K. Huang. 2012. 'JNK3 perpetuates metabolic stress induced by Abeta peptides', *Neuron*, 75: 824 − 37.
38. Yoshida, H., C. J. Hastie, H. McLauchlan, P. Cohen, and M. Goedert. 2004. 'Phosphorylation of microtubule-associated protein tau by isoforms of c-Jun N-terminal kinase (JNK)', *J Neurochem*, 90: 352 − 58.

39. You, L., X. Wang, W. Wu, E. Nepovimova, Q. Wu, and K. Kuca. 2022. 'HIF-1alpha inhibits T-2 toxin-mediated "immune evasion" process by negatively regulating PD-1/PD-L1', *Toxicology*, 480: 153324.
40. Zhang, C. C., A. Xing, M. S. Tan, L. Tan, and J. T. Yu. 2016. 'The Role of MAPT in Neurodegenerative Diseases: Genetics, Mechanisms and Therapy', *Molecular Neurobiology*, 53: 4893 – 904.
41. Zhang, C., J. Zhan, M. Zhao, H. Dai, Y. Deng, W. Zhou, and L. Zhao. 2019. 'Protective mechanism of Taxifolin for chlorpyrifos neurotoxicity in BV2 cells', *Neurotoxicology*, 74: 74–80.
42. Zhang, X., K. Zhou, R. Wang, J. Cui, S. A. Lipton, F. F. Liao, H. Xu, and Y. W. Zhang. 2007. 'Hypoxia-inducible factor 1alpha (HIF-1alpha)-mediated hypoxia increases BACE1 expression and beta-amyloid generation', *J Biol Chem*, 282: 10873-80.
43. Zhang, Z., J. Yan, Y. Chang, S. ShiDu Yan, and H. Shi. 2011. 'Hypoxia inducible factor-1 as a target for neurodegenerative diseases', *Curr Med Chem*, 18: 4335-43.
44. Zhao, Y., K. Kuca, W. Wu, X. Wang, E. Nepovimova, K. Musilek, and Q. Wu. 2022. 'Hypothesis: JNK signaling is a therapeutic target of neurodegenerative diseases', *Alzheimers Dement*, 18: 152 – 58.

Figures

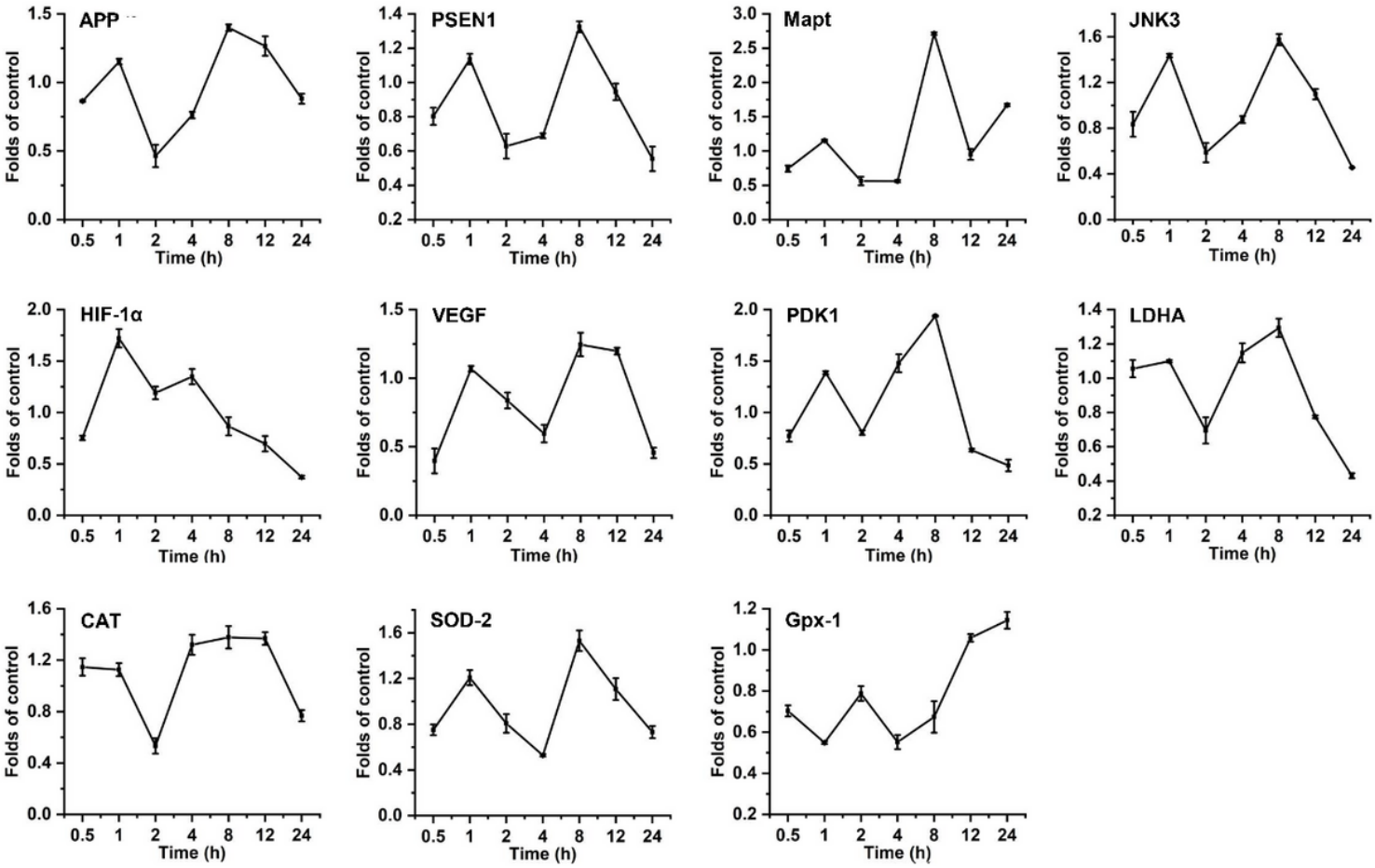

Figure 1

The kinetics of expression of key genes in cells treated for 0.5-24 h with T-2 toxin (8 nM). T-2 toxin caused significant expression of *APP*, *PSEN1*, *Mapt*, *JNK3*, *VEGF*, *PDK1*, *LDHA*, *CAT* and *SOD-2* at 8 h. *HIF-1α*expression was highest at 1h. *Gpx-1* was significantly expressed at 1h, then declined, and continued to rise after 4 h until 24 h. Data were presented as mean ± SD (n=3).

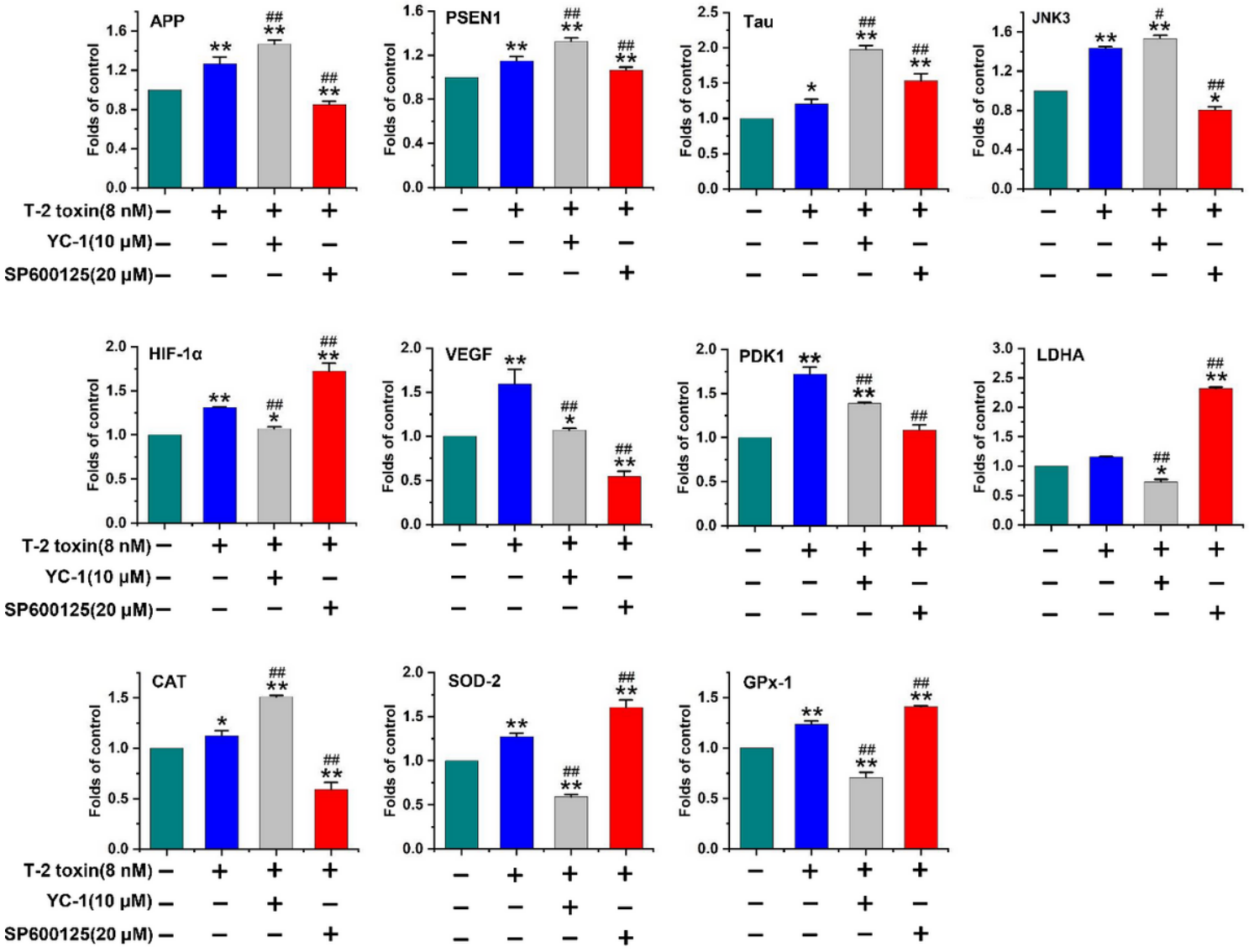

Figure 2

The effect of different inhibitors on the expression of key genes mediated by T-2 toxin (8 nM). T-2 toxin was applied to the cells for 8 h after inhibitors (SP600125 or YC-1) had worked on the cells for 1 h. Data were presented as mean ± SD (n=3). *APP*: $F_{3,8}$=84.416, *PSEN1*: $F_{3,8}$=136.761, *Mapt*: $F_{3,8}$=91.045, *JNK3*: $F_{3,8}$=4528.313, *HIF-1α*: $F_{3,8}$=78.896, *VEGF*: $F_{3,8}$=2281.934, *PDK1*: $F_{3,8}$=2281.934, *LDHA*: $F_{3,8}$=72.831, *CAT*: $F_{3,8}$=4350.687, *GPx-1*: $F_{3,8}$=286.88, *SOD-2*: $F_{3,8}$=165.814. *p<0.05, **p<0.01 vs. control group; #p<0.05, ##p<0.01 vs. toxin group.

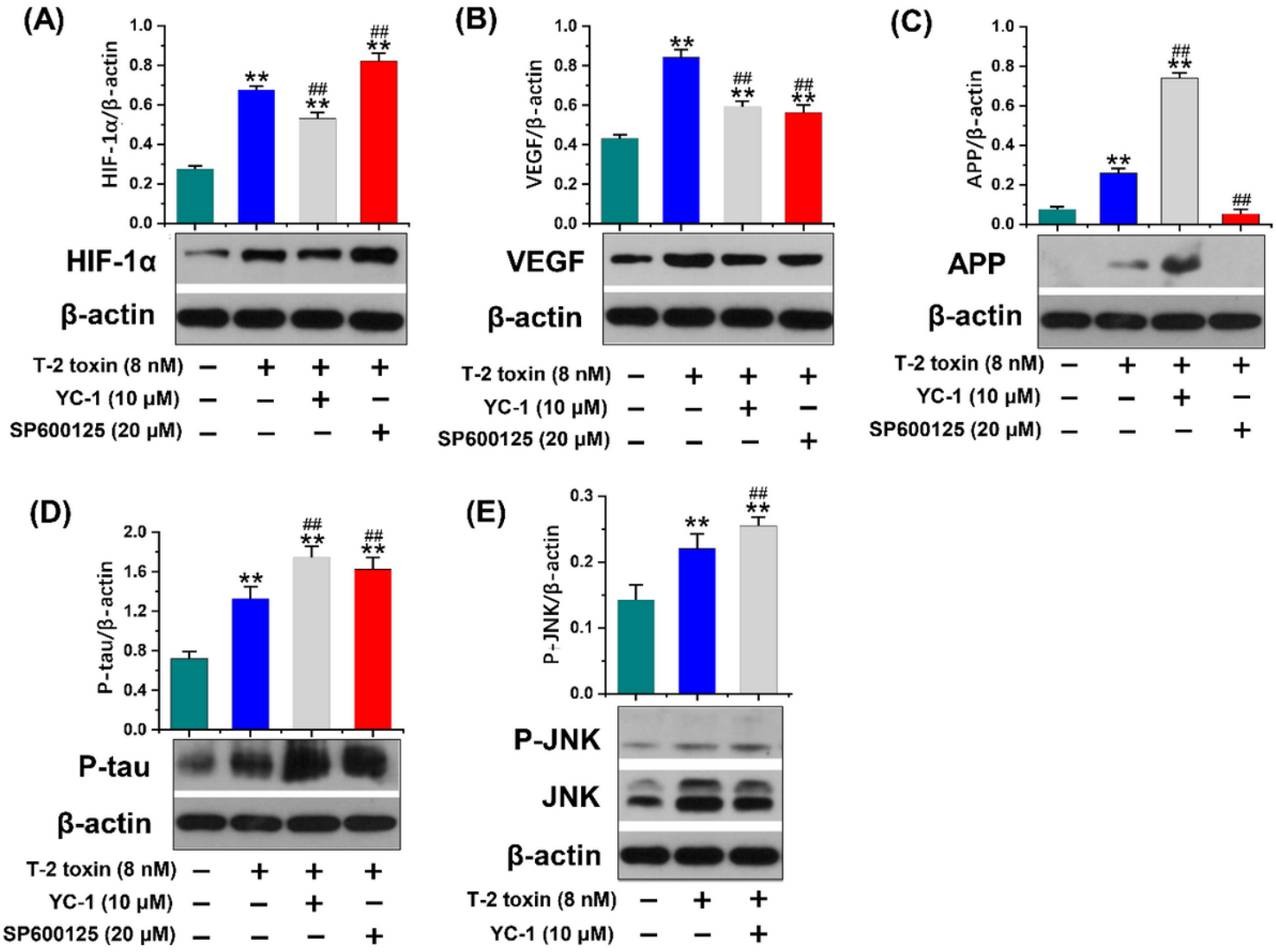

Figure 3

The effect of various inhibitors on the protein expression of HIF-1α (A), VEGF (B), Aβ (C), P-tau (phospho T181) (D), and P-JNK (E) mediated via T-2 toxin (8 nM). T-2 toxin was applied to the cells for 8 h after inhibitors (SP600125 or YC-1) had worked on the cells for 1 h. Data were presented as mean ± SD (n=3). HIF-1α: $F_{3,8}$=10772.937, VEGF: $F_{3,8}$=1192.786, Aβ: $F_{3,8}$=30588.838, P-tau: $F_{3,8}$=14393.209, JNK: $F_{2,6}$=1041.529. *p<0.05, **p<0.01 vs. control group; #p<0.05, ##p<0.01 vs. toxin group.

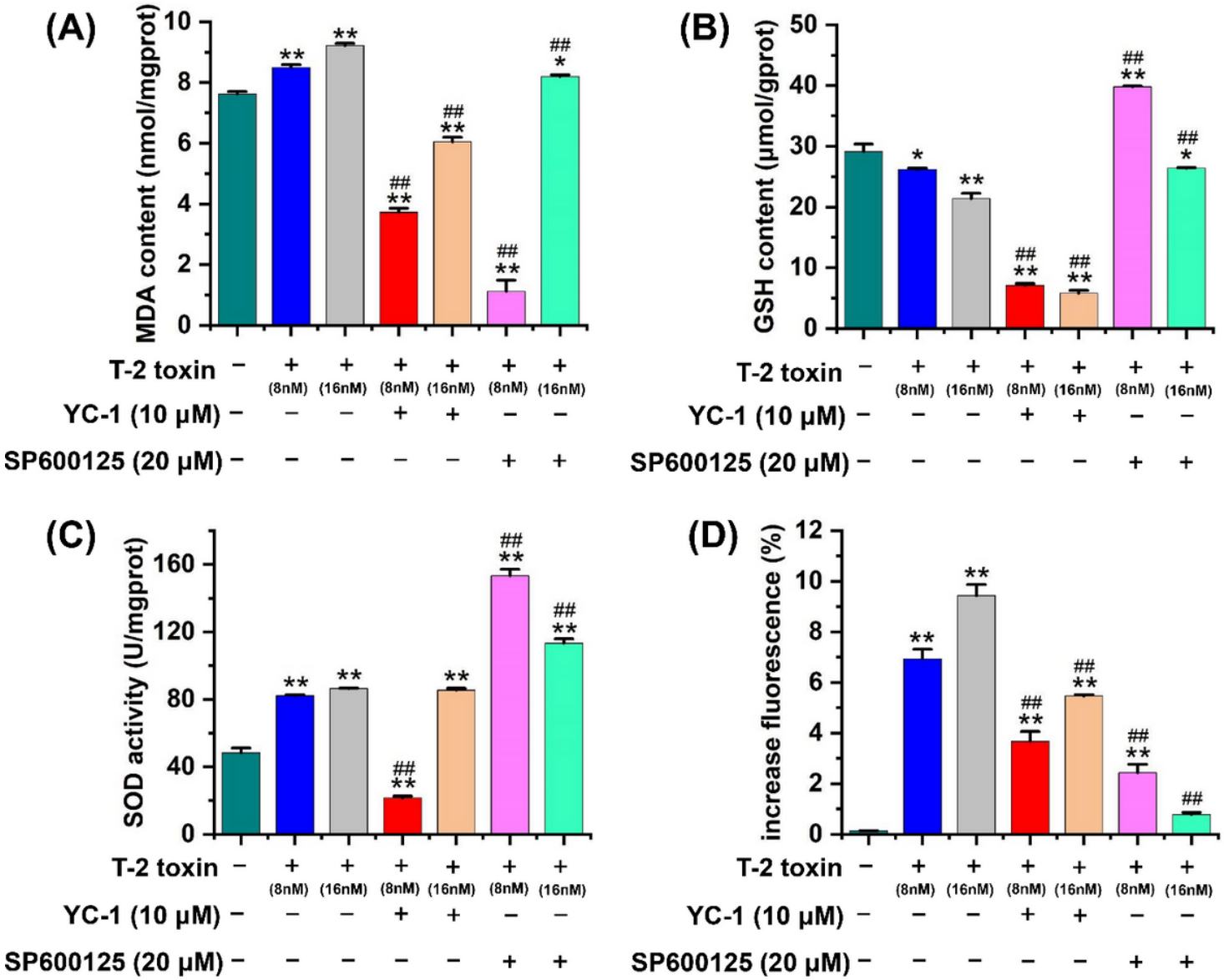

Figure 4

Effects of T-2 toxin on levels of MDA (A), GSH (B), SOD (C), and ROS (D) in BV2 cells when pathway inhibitors were present. T-2 toxin (8 or 16 nM) was applied to the cells for 8 h after inhibitors (SP600125 or YC-1) had worked on the cells for 1 h. Data were presented as mean ± SD (n=3). MDA: $F_{6,14}$=659.421, GSH: $F_{6,14}$=880.529, SOD: $F_{6,13}$=1170.151, ROS: $F_{6,14}$=400.782. *p<0.05, **p<0.01 vs. control group; #p<0.05, ##p<0.01 vs. toxin group.

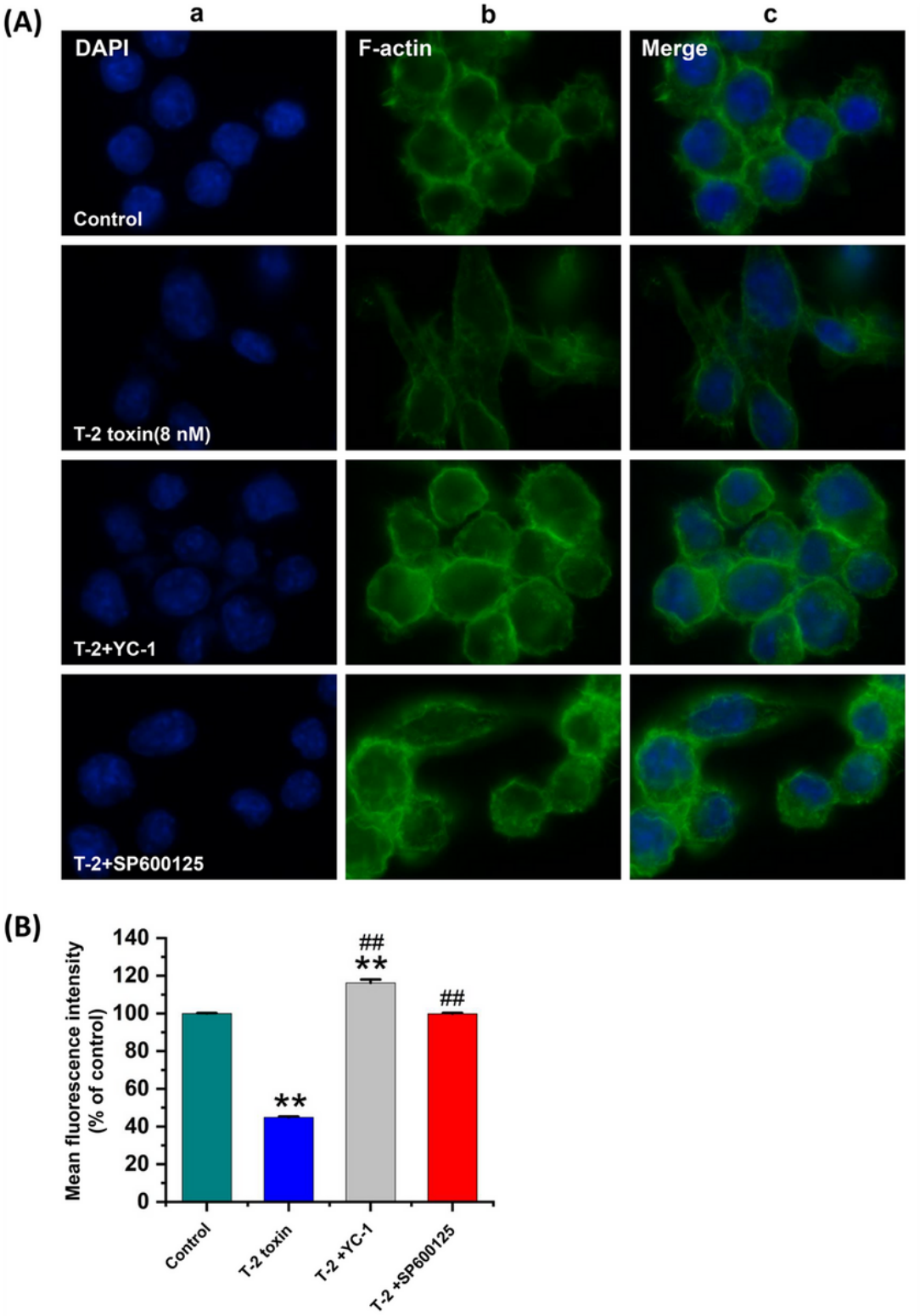

Figure 5

Effects of T-2 toxin on cytoskeleton under the influence of different inhibitors. T-2 toxin (8 nM) was applied to the cells for 8 h after inhibitors (SP600125 or YC-1) had worked on the cells for 1 h. Column a: DAPI nuclear staining. Column b: Filamentous actin (F-actin) of the cytoskeleton labeled with phalloidin. Column c: coincidence of nuclei and F-actin. (A): YC-1 and SP600125 were effective in blocking the destruction of cytoskeleton by T-2 toxin. (B): the ratio of F-actin fluorescence intensity before and after

YC-1 and SP600125 treatment cells to the control group. Data were presented as mean ± SD (n=3). *p<0.05, **p<0.01 vs. control group; #p<0.05, ##p<0.01 vs. toxin group.

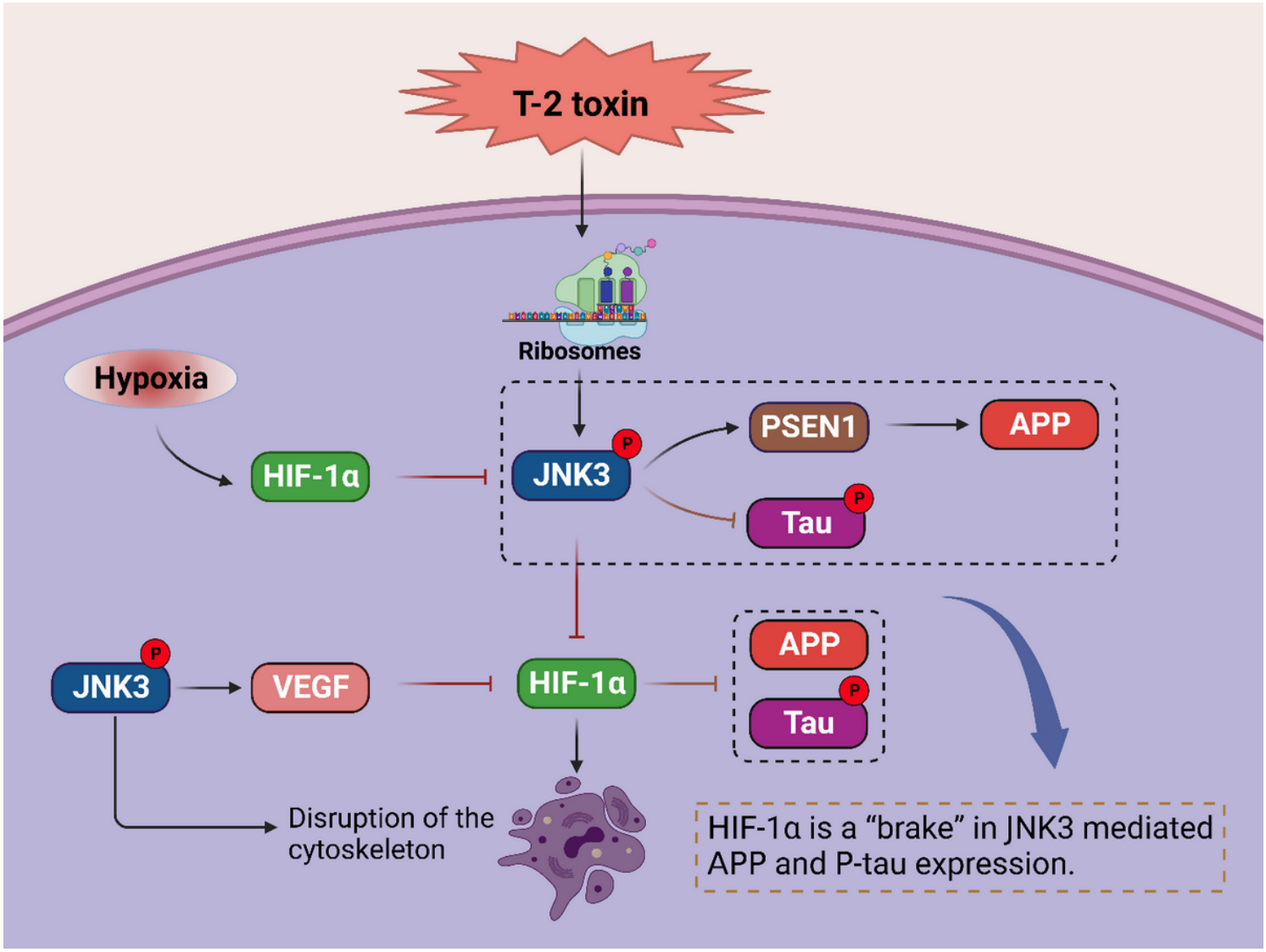

Figure 6

Mechanisms of HIF-1α and JNK signaling in Aβ and P-tau expression caused via T-2 toxin. HIF-1α signaling can be rapidly activated via T-2 toxin and prevents T-2 toxin-induced Aβ and P-tau expression. However, JNK3 breaks this inhibition (the inhibitory effect of HIF-1α) and finally promotes the formation of APP and P-tau.